Optical Nature of Non-Substituted Triphenylmethyl Cation: Crystalline State Emission, Thermochromism, and Phosphorescence

Tomohiko Nishiuchi,*[a,b] Hikaru Sotome,[c] Risa Fukuuchi,[d,e] Kenji Kamada,[d,e] Hiroshi Miyasaka,[c] and Takashi Kubo *[a,b]

[a] Dr. T. Nishiuchi, Prof. Dr. T. Kubo
Department of Chemistry, Graduate School of Science, Osaka University, 1-1 Machikaneyama, Toyonaka, Osaka 560-0043, Japan
E-mail: nishiuchit13@chem.sci.osaka-u.ac.jp
[b] Dr. T. Nishiuchi, Prof. Dr. T. Kubo
Innovative Catalysis Science Division, Institute for Open and Transdisciplinary Research Initiatives, (ICS-OTRI), Osaka University, Suita, Osaka 565-0871, Japan
[c] Dr. H. Sotome, Prof. Dr. H. Miyasaka
Division of Frontier Materials Science and Center for Advanced Interdisciplinary Research, Graduate School of Engineering Science, Osaka University, Toyonaka, Osaka 560-8531, Japan
[d] Ms. R. Fukuuchi, Prof. Dr. K. Kamada
Nanomaterial Research Institute (NMRI), National Institute of Advanced Industrial Science and Technology (AIST), Ikeda, Osaka 563-8577, Japan.
[e] Ms. R. Fukuuchi, Prof. Dr. K. Kamada
Department of Chemistry, Graduate School of Science and Technology, Kwansei Gakuin University, Sanda, Hyogo 669-1337, Japan

Keywords: carbocation, aggregation induced emission, crystal phase transition, thermochromism, phosphorescence

Abstract: Since the discovery of the triphenylmethyl (trityl) cation 120 years ago, a variety of aromatic cations having various colors and luminescence properties have been rigorously studied. Many, differently substituted trityl cations have been synthesized and their optical properties have been elucidated. However, the optical properties of the parent, non-substituted and highly reactive trityl cation, which was observed to be very weakly luminescent, have not been subjected to detailed investigation. In the effort described herein, we explored the optical nature of non-substituted trityl hexafluorophosphate (PF_6) in the crystalline state. Trityl PF_6 was found to exist as two crystal polymorphs including a yellow (**Y**) and an orange (**O**) form. Moreover, we observed that these crystalline forms display crystalline-state emission with different colors. The results of X-ray crystallographic analysis showed that the two polymorphs

have totally different molecular packing arrangements. Furthermore, an investigation of their optical properties revealed that the **O**-crystal undergoes a distinct color change to yellow upon cooling as a consequence of a change in the nature of the charge transfer interaction between the cation and PF_6 anion, and that both the **Y**- and **O**-crystal exhibit phosphorescence.

Introduction

Triphenylmethyl (trityl) cation[1-4] is a classical carbocation that possesses three-fold symmetry and a positive charge that is delocalized over the entire molecule (Figure 1a). Trityl cation, which can be readily prepared by treatment of trityl alcohol with acid, exhibits intense absorption in the visible region. Since the time of the discovery of this cation, organic chemists have conducted extensive studies concentrating on the synthesis and exploration of derivatives including π-extended analogs[5-8] and heteroatom containing (N or O) systems, as well as on developing methods for stabilizing the cationic state toward reactions with nucleophiles, and tuning its absorption and emission properties. Through these efforts, many highly absorbing and emitting derivatives have been uncovered, including those of malachite green, crystal violet, fluorescein and rhodamine derivatives that are utilized as textile dyes, external stimuli responsiveness fluorescent probes and cell imaging reagents[9-11] (Figure 1b). Furthermore, owing to its high reactivity, the non-substituted (NS) trityl cation has been widely used as a Lewis acid catalyst (Mukaiyama-type aldol or Michael reaction), photooxidation promoter, hydride acceptor and protecting group component.[12-16] In contrast, the optical properties of NS trityl cation have not yet been fully explored likely because of its high reactivity.

Although various new aromatic compounds have been synthesized, knowledge about the fundamental properties of reactive aromatic cations is also useful in the development of cationic dye, sensors and emissive materials. It seems appropriate, that now, 120 years from the time of the first report of the trityl cation,[2,3] we have carried out an investigation exploring the absorption and luminescence features of the NS trityl cation. In this effort, we discovered that

in the crystalline state NS trityl cation displays bright luminescence, unique thermochromism,[17-20] and phosphorescence[21-25] which are governed by the arrangement of molecules in the crystal.

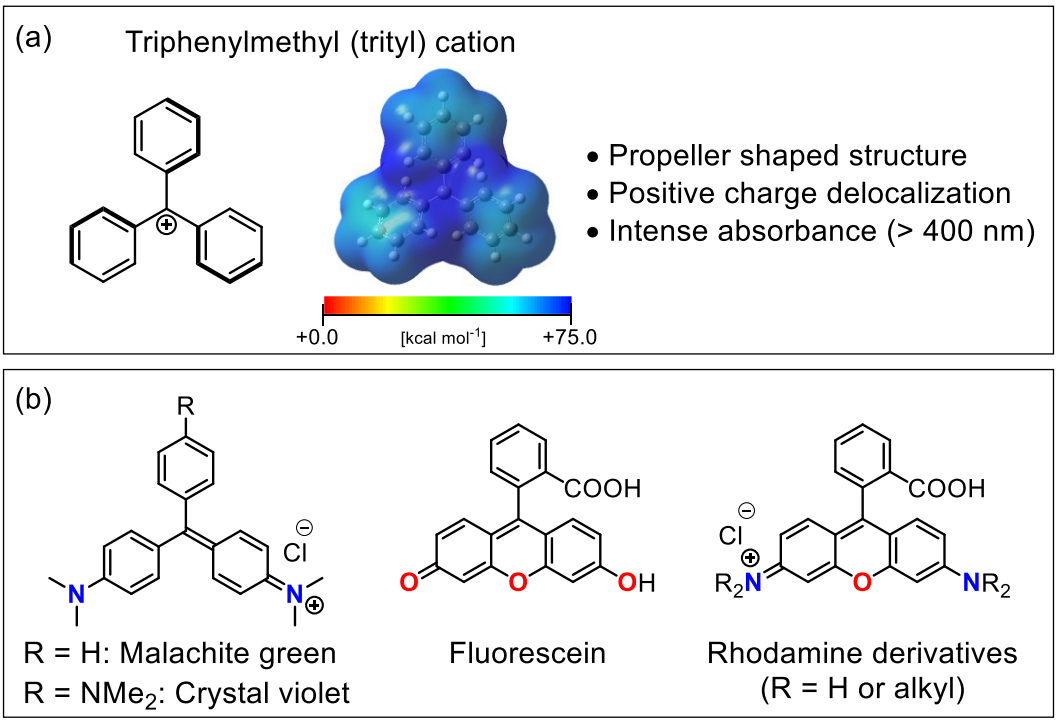

Figure 1. (a) Structure of NS trityl cation and electrostatic potential surface (B3LYP/6-31G**). (b) Trityl cation based stable dye, fluorescent probe, or emissive imaging materials containing heteroatoms.

Results and Discussion

Synthesis and crystallization behavior

The NS trityl cation with PF_6 as the counter anion was prepared by treatment of trityl alcohol with hexafluorophosphoric acid (HPF_6). Specifically, to a solution of trityl alcohol in acetic anhydride at room temperature was added a 60% HPF_6 and the resulting mixture was let stand at room temperature while crystal growth occurred.[26] At first, yellow (**Y**) crystals formed (Figure 2a, b), but when the solution stood for a several ten minute period, production of orange (**O**) crystal began (Figure 2c, 2d). Finally, upon standing for days to weeks (Figure 2e-2g), **O**-

crystal are formed as the major component. Different from single-crystal-to-single-crystal transition,[27-32] this crystal phase transition from **Y**- to **O**-crystal requires a seed nuclei of **O**-crystal and the transition started from a contact point with **O**-crystal. In addition, the crystal phase transition can be effectively suppressed by keeping the solution at low temperature (4 °C). This phenomenon enabled selective isolation of the two crystal polymorphs.

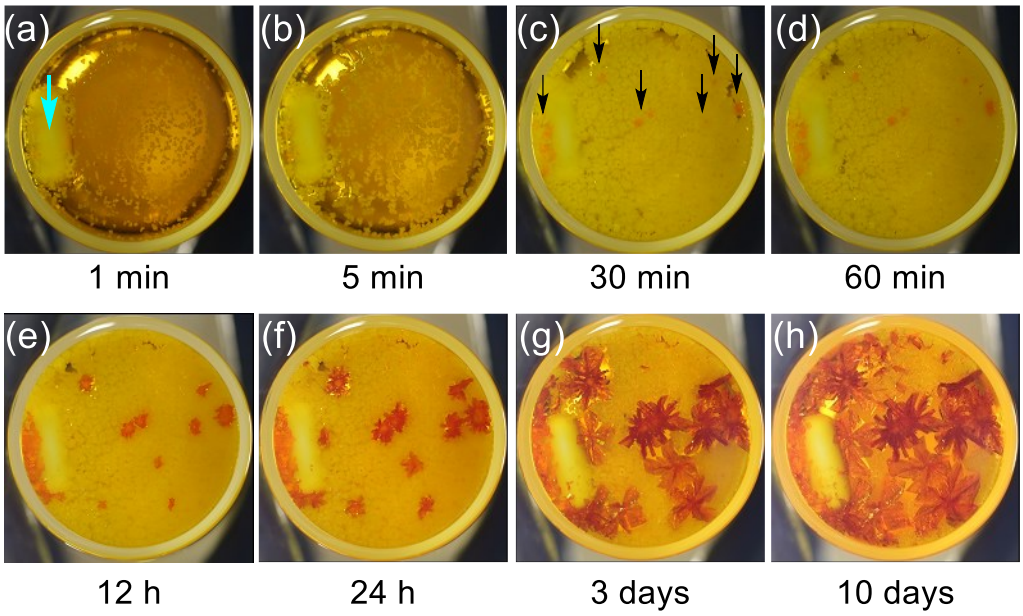

Figure 2. Photographs showing crystal growth and a SCSC phase transition from (a) **Y**-crystal to (h) **O**-crystal at elapsed times following initiation of crystallization. The blue arrow in (a) indicates a stir tip as a standard material. The black arrows in (c) indicate the beginning of growth of the **O**-crystal.

It was known that the colors of trityl salts in the solid state varied with the counter anion but the reason have not yet been fully investigated. It was previously reported that the crystal color of trityl PF_6 is orange.[33] Furthermore, trityl tetrafluoroborate, prepared to evaluate the counter anion effect on the crystal phase transition, was found not to exist as crystal polymorphs but only one yellow crystalline form, which has cell parameters that are similar to those of the with **Y**-crystal of trityl PF_6 (Figure S5). Thus, the nature of the counter anion is crucial for the occurrence of this crystal phase transition. The thermal stabilities of the **Y**- and **O**-crystals were elucidated by using differential scanning calorimetry (DSC). The scan of the **Y**-crystal contains lower endothermic peaks at 104 °C (phase transition) and 183 °C (melting

point) and that of **O**-crystal contains a peak at 259 °C (decomposition) (Figure S1). In addition, X-ray analysis shows that the calculated crystal density of the **O**-crystal at 273 K is 1.524 g cm^3, which is higher than that of the Y-crystal (1.413 g cm^3). These results indicate that formation of the **Y**-crystal phase is kinetically preferred and the **O**-crystal is thermally more stable in a manner that typically exemplifies the Ostwald's step rule.[34-36]

Optical properties and crystal structures

In Figure 3a are shown the UV-vis spectrum of the NS trityl cation in $CHCl_3$ solution, generated by reaction of trityl alcohol with 2% TFA, and solid-state transmission UV-vis spectra of **Y**- and **O**-crystals dispersed in KBr pellets. The color of the solution of the trityl cation is yellow, corresponding to a λ_{max} at 435 and 410 nm (ε = 45000 cm^{-1} M^{-1}). The UV-vis spectrum of the **Y**-crystal is nearly identical to that of a solution of the trityl cation whereas the spectrum of the **O**-crystal contains a distinctively bathochromically shifted maximum above 550 nm. This finding was also confirmed by inspection of the solid-state diffuse reflectance spectra of these crystals (Figure S2). Although several aromatic cations containing heteroatoms such as N or O are known to exhibit intense emission,[37,38] those composed of only hydrogen and carbon exhibit very weak or no emission in solution owing to the favorability of non-radiative decay processes.[39] In fact, the trityl cation in solution displays no emission. On the other hand, both the **Y**- and **O**-crystals of trityl PF_6 display relatively intense yellow green (λ_{em} = 525 nm) and orange (λ_{em} = 585 nm) emission, respectively (Figure 3b). The emission quantum yields of the **Y**- and **O**-crystals at 293 K are 4% and 12%, respectively. This phenomenon is a consequence of aggregation induced emission (AIE)[40-48] because non-radiative decay associated with rotation of the three phenyl rings is effectively suppressed in the crystalline state. To the best of our knowledge, no hydrocarbon cations and only a few aromatic cations containing N and O atoms have been reported to exhibit AIE.[23,48]

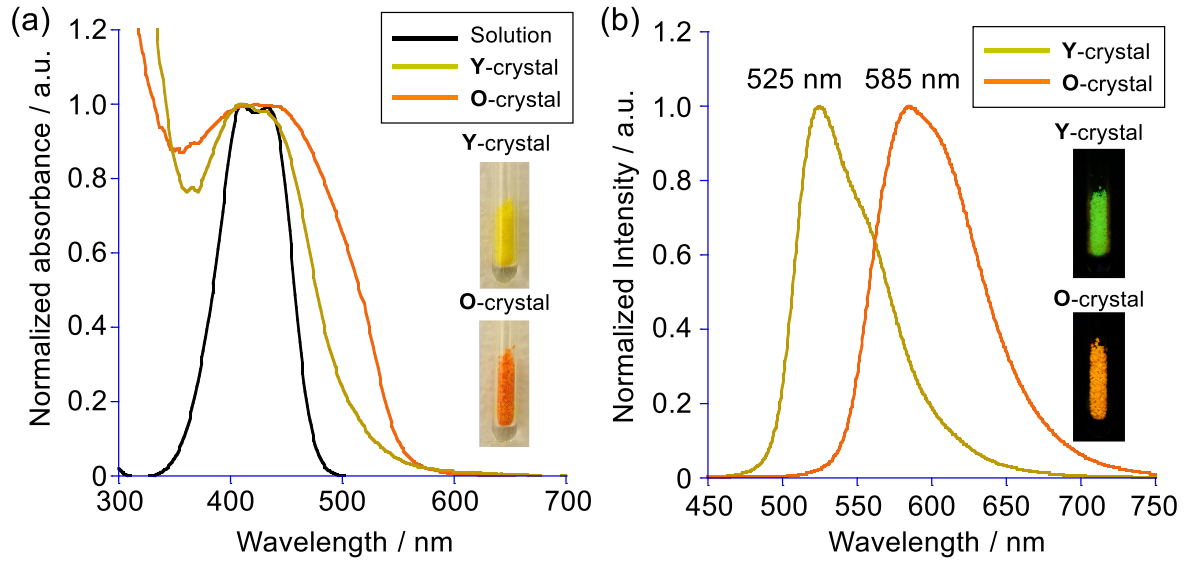

Figure 3. (a) UV-vis spectrum of trityl cation (2% TFA in $CHCl_3$) and solid-state UV-vis spectra of **Y**- and **O**-crystals (KBr pellet). (b) Emission spectra of **Y**- and **O**-crystals (λ_{ex} = 360 nm).

To gain information about the optical differences between the **Y**- and **O**-crystals, single crystal X-ray analysis was performed to determine crystal packing structures. The results show that the trityl cation in the **Y**-crystal at 170 K has D_3 symmetry with a torsion angle of the three phenyl rings being 32.9° (Figure 4a and Table S1). The **Y**-crystal shows a space group, $F4_132$, and the asymmetric unit contains 1/6 of trityl cation. Therefore, the unit cell contains 16 trityl cations clustered in four sets within each sets trityl cations are tetrahedrally arranged (Figure 4b) and the PF_6 anions are located in a central cavity as well as in areas surrounding the tetrahedron (Figure 4c). Thus, each trityl cation in the **Y**-crystal is completely isolated from neighboring cations by intervening PF_6 anions and, as a result, no significant interactions exist between the trityl scaffolds. As stated above, the molecular arrangement in the **Y**-crystal is reflected in its UV-vis spectrum, which is similar to that of the solution state.

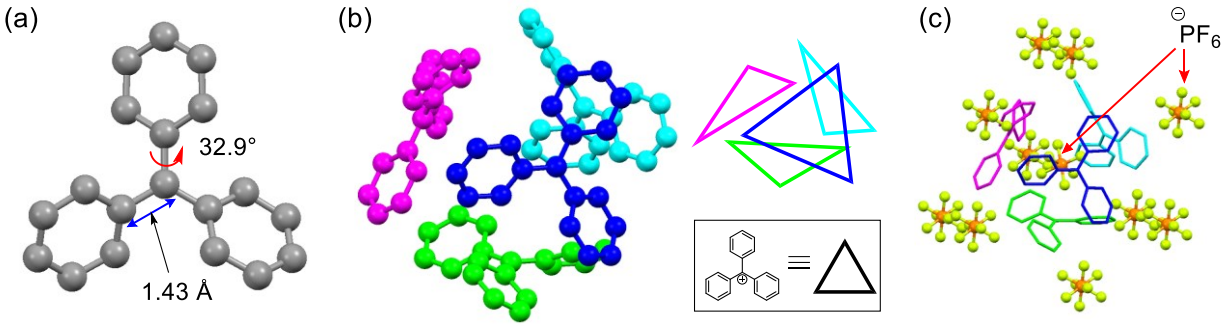

Figure 4. X-ray crystallographic analysis of **Y**-crystal (170 K). (a) Torsion angle of phenyl ring and C-C distance between central sp^2 carbon and phenyl ring. (b) Tetrahedral arrangement of trityl cations depicting different colors without PF_6 anions for clarity (left) and schematic drawing of the tetrahedral arrangement of trityl cations (right). (c) Drawing with PF_6 anions shown in (b). Protons are omitted for clarity.

In a manner that is different from that of the in the **Y**-crystal, the trityl cation scaffold in the **O**-crystal has C_1 symmetry with the different torsion angles between the three phenyl rings being 25.4, 31.8 and 40.2° (Table S2). Two types of aggregation arrangements exist in the packing structure of the **O**-crystal. In one of these, two trityl cations form a face-to-face dimer with PF_6 anions at exterior positions (Figure 5a, b). The intermolecular atomic distance between the central sp^2 carbon of the trityl cations is 4.265 Å (195 K), which is *ca.* 1.0 Å greater than the distance for typical π-π stacking. In the other arrangement, the trityl cations are one dimensionally laterally aligned with a periodic distance of 8.698 Å (Figure 5c).[49] It is noteworthy that the inter-atomic C···F distance between central sp^2 carbon of the trityl cation and fluorine atom in PF_6 anion is 3.101 Å (195 K) (Figure 5b), a value that is almost identical to the sum of the van der Waals (vdWs) radii of carbon (1.70 Å) and fluorine (1.47 Å) atoms. This observation indicates the existence of a stronger anion-π^+ interaction [50-53] than that existing in the **Y**-crystal (C···F distance is 3.503 Å at 170 K). In fact, the results of natural bond orbital (NBO) analysis of trityl PF_6 monomer in both **Y**- and **O**-crystals using MP2/6-311+G** reveals that a charge-transfer (CT) interaction is present between the trityl cation and PF_6 anion[50] and that the degree of the CT interaction in the **O**-crystal is larger than it is in the **Y**-crystal (Figure S8). In addition, the NBO analysis suggests that the face-to-face trityl PF_6

dimeric structure in **O**-crystal enables a greater degree of CT interaction than that which exists in the trityl PF_6 monomer (Figure S9). This is likely caused by the unfavorable cation-cation repulsive energy in the face-to-face dimeric structure which enhances CT interaction from the PF_6 anion to the trityl cation.

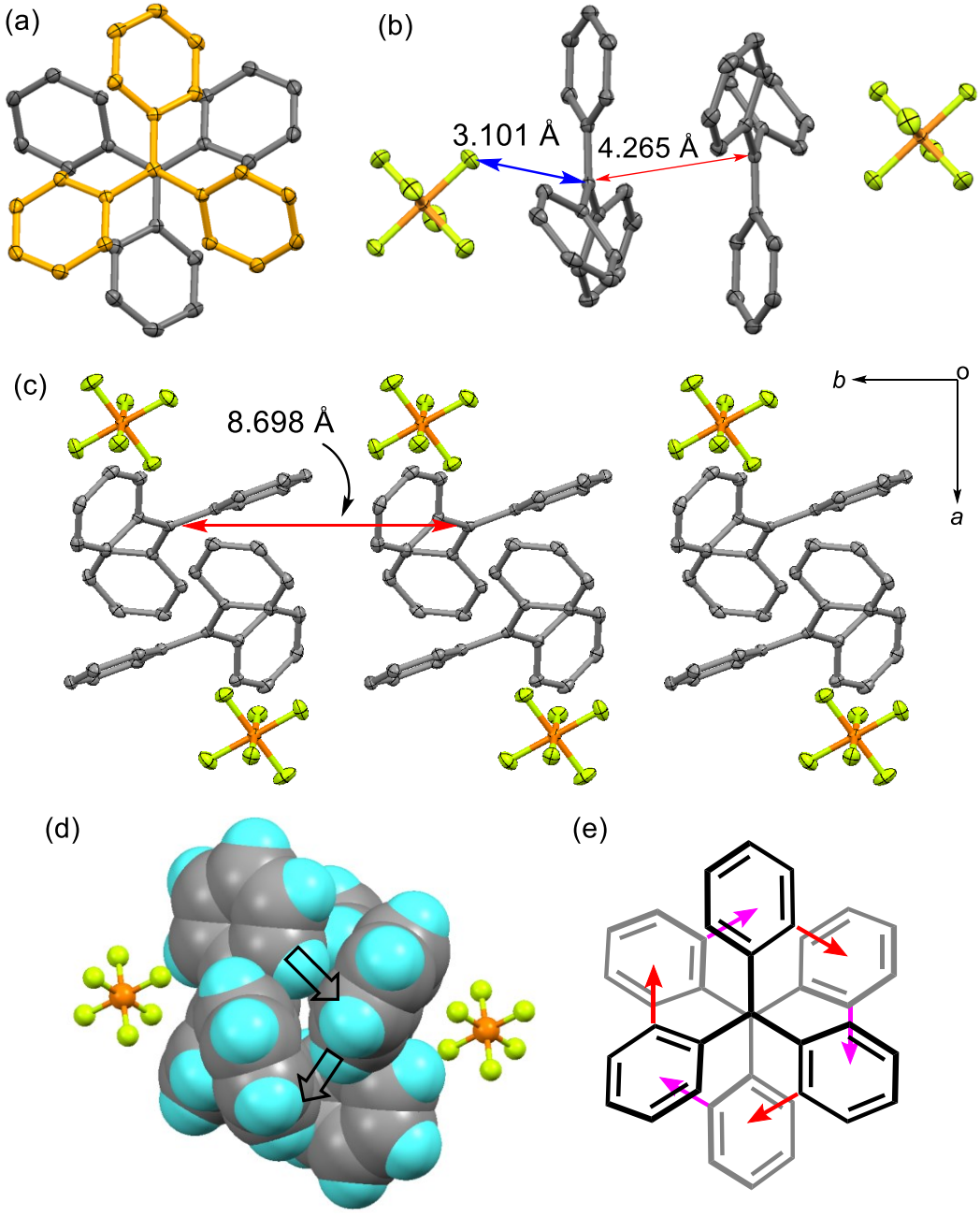

Figure 5. X-ray crystallographic analysis of **O**-crystal (195 K). (a) Top view of trityl cation dimer in **O**-crystal with different colors and without PF_6 anions for clarity. (b) Side view of trityl PF_6 dimer in **O**-crystal with PF_6 anions. (c) One dimensional alignment of trityl PF_6 (viewing from *c* axis). Protons are omitted for clarity. Ortep drawing is 50% probability. (d) Six-fold phenyl embrace between the trityl cation represented by CPK model (trityl cations). (e) Schematic drawing of the edge-to-face interactions representing by red and pink arrows from axial view.

Furthermore, between the face-to-face trityl cation dimer, phenyl groups in both trityl cations possessed six-fold edge-to-face interactions (Figure 5d, e).[54] This interaction mode is known as six-fold phenyl embrace (SPE), which was first observed in triphenyl phosphine and tetraphenyl phosphonium cation, possessing a tetrahedral molecular shape.[55-57] To evaluate whether significant interactions work at between the face-to-face trityl cations, DFT calculations were performed to estimate the complexation energy using counterpoise method with BSSE correction (Figure S10). A repulsive complexation energy at +35.0 kcal mol^{-1} was observed when there is only two trityl cations whereas an attractive complexation energy at -10.6 kcal mol^{-1} was observed when PF_6 anions are included in the calculations. It is surprising that although the trityl cation has a triangle molecular shape which seems less favorable to form SPE arrangement than a molecule having tetrahedral shape, this complexation energy at -10.6 kcal mol^{-1} is close those of tetrahedral molecules (-14 to -20 kcal mol^{-1}).[55,57] Their electrostatic potential surfaces also revealed that the positive charged surface on trityl cation skeleton is significantly reduced by the existence of PF_6 anion (Figure S11). Therefore, the CT interaction from PF_6 anion is crucial to form the SPE between the triangle molecular shape of trityl cation scaffolds.[58]

Thermochromism of O-crystal

Additional investigations led to the discovery of other interesting properties of the **O**-crystal of trityl PF_6. Upon cooling the temperature from room temperature to 77 K the color of **O**-crystal changed to yellow and the orange color reformed upon warming to room temperature (Figure 6a and Movie S1). Similar to these absorption changes, the emission color of **O**-crystal changes from orange to yellow orange upon cooling (Movie S2). This type of distinctive thermochromism does not take place with the **Y**-crystal (Movie S3-4, Figure S12). The thermochromic behavior of the **O**-crystal was evaluated by using emission and excitation

spectroscopic measurements (Figure 6b, c). The excitation spectrum at room temperature contains a peak at 560 nm whereas at 77 K the maximum occurs at a wavelength shorter than 560 nm. In addition, the emission peak also shifts from 585 nm to 560 nm when the temperature is lowered from room temperature to 77 K.

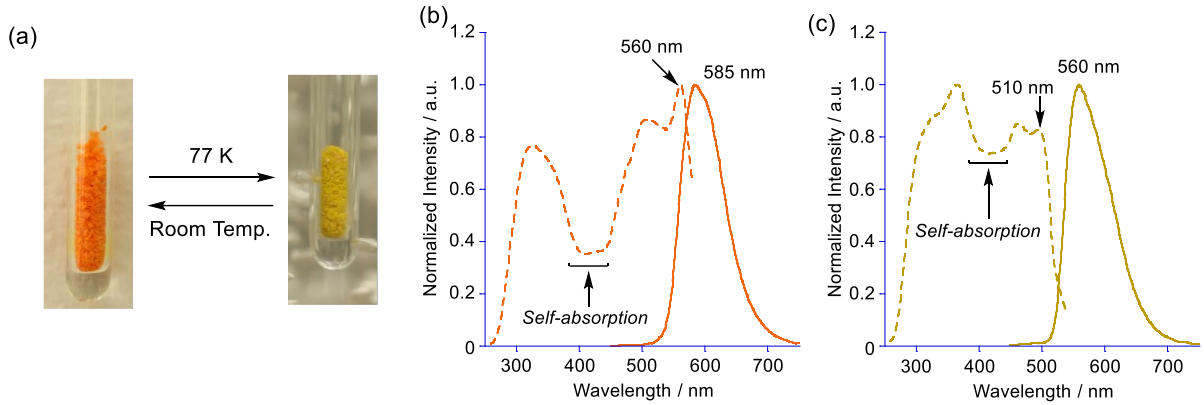

Figure 6. (a) Thermochromism of the **O**-crystal between room temperature and 77 K. The detail of this thermochromism can be seen in Movie S1 (under room light) and Movie S2 (under UV light). (b) Excitation (dash line) and emission (solid line) spectra of **O**-crystal at 293 K. (c) Excitation (dash line) and emission (solid line) spectra of **O**-crystal at 77 K. In both excitation spectra, self-absorption from 400 to 450 nm is due to the intense absorption on the crystal surface. (λ_{ex} = 360 nm for emission measurements, λ_{em} = 585 nm in 293 K and λ_{em} = 560 nm in 77 K for excitation measurements.)

To evaluate the relationship between thermochromism and structural changes, single crystal X-ray analysis was conducted on the **O**-crystal at 273 and 83 K (Figure S6, S7). The results show that upon cooling, no change occurs in the crystal system (monoclinic, $P2_1/n$) and negligible changes take place in the torsion angles of three phenyl rings, as well as in C-C bond lengths between the central sp^2 carbon and ipso-phenyl carbons (Table S2). On the other hand, the inter-atomic C···F distance between fluorine atom of the PF_6 anion and the central sp^2 carbon of trityl cation upon cooling shortens from 3.155 Å (273 K) to 3.047 Å (83 K) (Figure 7a and Figure S5, S6), which is shorter than the sum of vdWs radii of carbon and fluorine atoms. In addition, the distance between the central sp^2 carbons in face-to-face trityl cation dimers in the crystal are slightly reduced from 4.296 Å (273 K) to 4.232 Å (83 K) (Figure 7b) upon cooling. The cause of this change is reduction of the net charge on the trityl cation by strong

CT from the PF_6 anion, which is confirmed by using Hirshfeld atomic population analysis (MP2/6-311+G**, Table S3). On the other hand, no difference of the complexation energy of SPE in two trityl cation scaffolds was confirmed at between 273 K and 83 K (Figure S10).

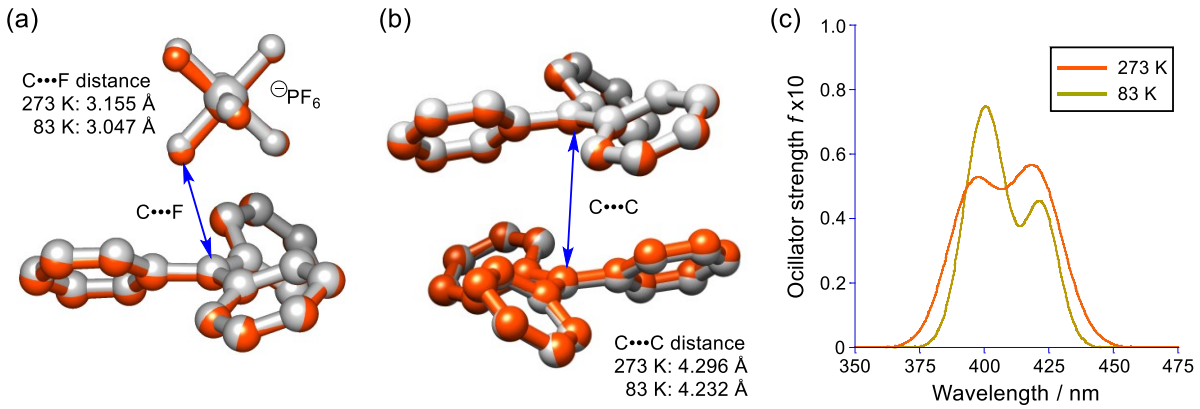

Figure 7. (a) Superposition of the structure generated by VT X-ray analysis of **O**-crystal at 273 K (grey) and 83 K (orange). Depicting the structural changes between PF_6 anion and trityl cation. (b) Depicting the structural changes between face-to-face trityl cation dimer. (c) TD-DFT simulated absorption spectra of trityl PF_6 dimer at 273 K (orange line) and 83 K (yellow line).

TD-DFT calculations of a trityl PF_6 ion pair and its dimers observed in the **O**-crystal at both 273 and 83 K were carried out using CAM-B3LYP functional with a tuned parameter method (μ = 0.150, α = 0.0799, β = 0.9201 (α + β = 1.0)) as developed by Nakano.[59] The calculated results of face-to-face trityl PF_6 dimer revealed that the longer wavelength transitions (430.4, 429.6 and 424.8 nm with respective f = 0.0004, 0.0035 and 0.0116, Table S4 and Figure S13) at 273 K are associated with a weak CT transition from the PF_6 anion to the trityl cation. The longer wavelength transition at 83 K corresponds to an intramolecular transition in trityl cation (422.0 nm, f = 0.0441) because shortening of the C···F distance leads to strengthen the CT transition and shifting it to higher energy (406.1, 404.3 and 402.7 nm with respective f = 0.0052, 0.0039 and 0.0438, Table S5 and Figure S14). Simulated absorption spectra of the trityl PF_6 dimer at 273 K and 83 K are well reproducing the blue-shift of absorption upon cooling as shown in **O**-crystal (Figure 7c and Figure S15). In contrast, TD-DFT calculations of a trityl PF_6

ion pair and a laterally arranged trityl PF_6 dimer show that little change occurs in the longer wavelength transition upon changing the temperature between 273 and 83 K (Table S6-S8 and Figure S16-22). Therefore, the face-to-face dimer structure promoted perturbation of the CT transition energy through a cation-cation repulsive interaction is the cause of the prominent color change from orange to yellow that occurs upon cooling the **O**-crystal.

Phosphorescence in trityl cation

The trityl cation is isoelectronic with triphenylborane, which displays unique optical properties including thermally activated delayed fluorescence (TADF).[60-65] Owing to this relationship, we explored the delayed emissive nature of trityl PF_6. The emission spectrum of a frozen state of trityl cation (5.0×10^{-6} M) in $CHCl_3$ with 2% TFA at 77 K contains a broad weak peak from 510 to 520 nm and an intense peak at 550 nm (Figure 8a). Delayed emission measurements (10 ms delay) show that the broad and weak 510-520 nm peak disappears and an intense emission band at 550 nm arises. It is noteworthy that the same sample at 195 K contains a broad delayed emission band 515 nm (Figure S23). The broad 510-520 nm and intense 550 nm peaks are assigned as respective fluorescence and phosphorescence of trityl cation. Thus, a remarkably small energy gap (ΔE_{ST}) of 0.15 eV exists between S_1 and T_1 of this substance. The lifetime of the phosphorescence of trityl cation is 310 ms (Figure S25) and the emission quantum yield is 40% (Table 1).

In contrast to those of the frozen state, the phosphorescence emission properties of the **Y**- and **O**-crystals are totally different. The steady-state (SS) emission spectrum of **Y**-crystal at 77 K contains an intense peak at 510 nm, which is nearly the same wavelength as that in the fluorescence spectrum of frozen state of trityl cation. The phosphorescence emission spectrum of the **Y**-crystal contains two peaks at 550 and 585 nm (Figure 8b) associated with an emission lifetime of 340 ms, which is comparable with that of the frozen state. On the other hand, the SS

emission spectral band of the **O**-crystal begins at 480 nm with a maximum at 560 nm. In addition, the SS emission spectrum overlaps with that of its phosphorescence spectrum (Figure 8c).[66] Although the trityl cation has a small ΔE_{ST}, the emission quantum yield of the **O**-crystal is enhanced by cooling (12% at 293 K to 24% at 77 K), which rules out the existence of TADF. Therefore, emission occurs from the triplet state as phosphorescence, as shown in the SS emission spectrum of the **O**-crystal at 77 K.

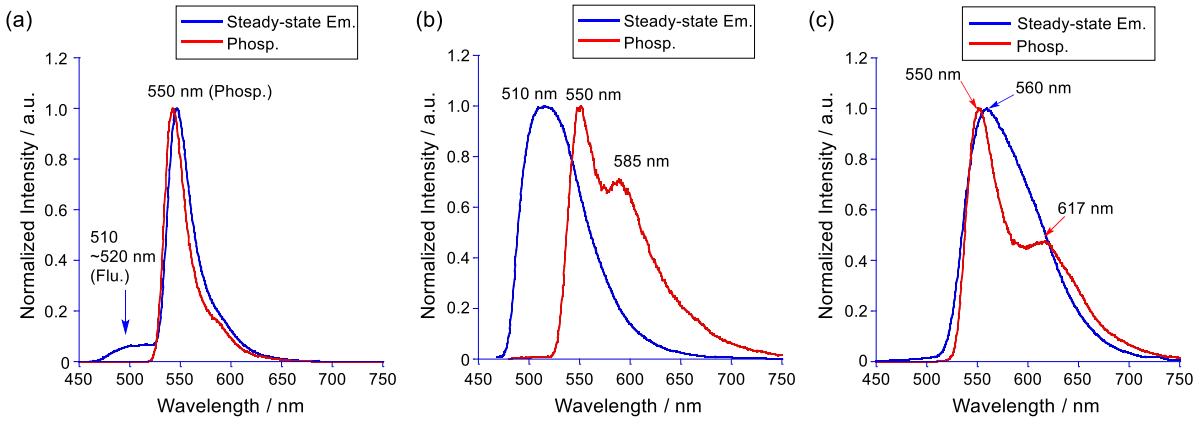

Figure 8. Steady-state emission and phosphorescence (10 ms delay, 8 ms integration) spectra at 77 K. (a) Frozen state ($CHCl_3$ with 2% TFA, 5.0 x 10^{-6} M) of trityl cation. (b) **Y**-crystal. (c) **O**-crystal. (λ_{ex} = 360 nm).

Table 1. Emission peaks, lifetime, and quantum yield of trityl cation (77 K), **Y**-crystal (293 and 77 K), and **O**-crystal (293 and 77 K).

	λ_{em} / nm	τ	Φ / % [d]
Trityl cation (77 K)[a]	510, 550	310 ms (550 nm)	40
Y-cryst. (293 K)	525	1.8 ns (525 nm)	4
Y-cryst. (77 K)	510 (SS)[b] 550, 585 (P)[c]	340 ms (550 nm)	11
O-cryst. (293 K)	585	9.1 ns (575 nm)	12
O-cryst. (77 K)	560 (SS)[b] 550, 617 (P)[c]	410 ms (560 nm)	24

[a]Trityl cation was generated from trityl alcohol in $CHCl_3$ with 2% TFA. [b] SS indicates steady-state emission. [c]P indicates phosphorescence emission.[d]Emission quantum yield contains both fluorescence and phosphorescence measured by using integrating sphere.

The emission lifetime of the **O**-crystal at 293 K is 9.1 ns (Figure S26) whereas at 77 K it is 410 ms, which is slightly longer than those of the frozen state and the **Y**-crystal. Longer wavelength emission peaks above 550 nm are present in the phosphorescence emission spectra of the **Y**-crystal (λ_{em} = 585 nm) and **O**-crystal (λ_{em} = 617 nm). Phosphorescence excitation spectra measured at 550 nm, 590 nm (for **Y**-crystal) or 620 nm (for **O**-crystal), were analyzed. Interestingly, excitation spectra measured at 550 nm in both crystals showed a similar shape with that of the absorption spectrum of trityl cation in solution whereas sharp longer wavelength shifted excitation spectra of both the **Y**- and **O**-crystal were observed at 590 and 620 nm excitation, respectively (Figure 9). Furthermore, excitation at 480 nm for **Y**-crystal and 500 nm for **O**-crystal leads to selected enhancements of the emission peaks at 580~585 nm for **Y**-crystal and 620 nm for **O**-crystal. On the other hand, the emission spectrum of the frozen state displays no dependence on excitation wavelength and concentration (Figure S24). Therefore, these longer wavelength phosphorescence peaks are attributed from their packing structures such as the arrangement of trityl cations whereas the emission peak at 550 nm is attributed from the monomer structure of trityl cation. Inspection of the ns to μs timescale emission decay profiles of the **Y**- and **O**-crystals at 77 K shows that, in contrast to the frozen state, both **Y**- and **O**-crystal display intense emission in nanosecond region (<240 ns) and relatively weak emission in microsecond region (Figure S27). Owing to the weakness of emission in the microsecond region, analysis of the long time decay up to the millisecond timescale was difficult to perform using our instrumental setup and, thus, the phosphorescence quantum yield could not be determined.

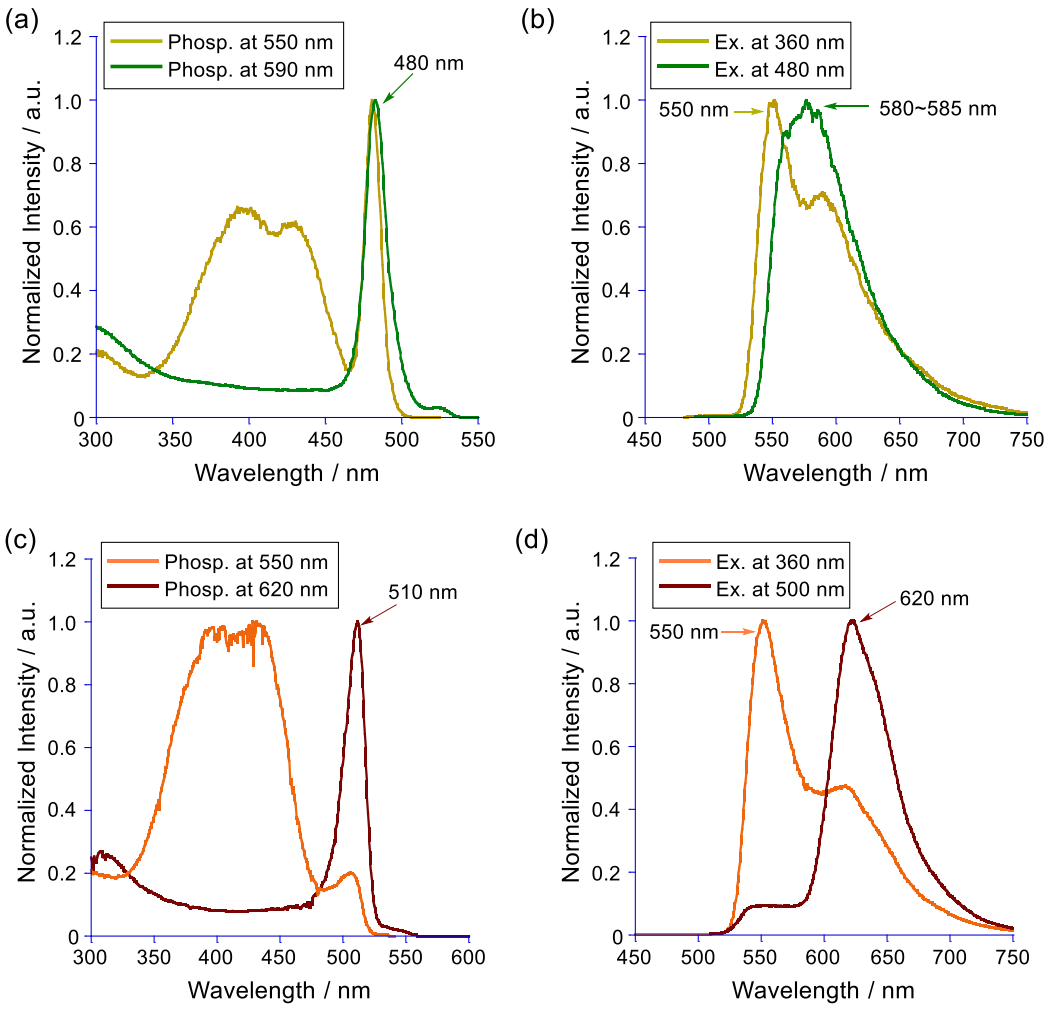

Figure 9. Phosphorescence excitation spectra and excitation wavelength dependence of phosphorescence of **Y**-crystal (a),(b) and **O**-crystal (c),(d). Spectra were measured with a 10 ms delay and 8 ms integration at 77 K.

Spin-orbit coupling (SOC) constants were calculated using the TD-DFT method with Tamm-Dancoff approximation (TDA) to evaluate the phosphorescence properties of the trityl cation. It is noteworthy that small SOCs occur between the S_0 and T_1 states as well as S_1 and T_n states of the trityl cation alone (Figure S28) whereas significant SOCs takes place between singlet and triplet states in the ion pair of trityl cation and PF_6 anion (Figure S29-S31). This finding indicates that ISC of the trityl cation is facilitated by the presence of the counter anion. Judging from the energies of the singlet and triplet excited states of trityl PF_6 ion pair in the **O**-crystal at 273 K, the energies of $S_{1,2}$, which are almost degenerated energy states, are close to

those of T_{6-8} and a large SOC exists between these states, resulting in effective ISC and enabling subsequent internal conversion T_{6-8} -> T_1.

The calculations also show that, although only small differences exist in the degree of SOC between trityl PF_6 ion pairs in the **Y**- and **O**-crystals as well as in the **O**-crystal between 273 and 83 K, a distinctive enhancement of the SOC exists in the face-to-face dimer of trityl PF_6 ion pair structure in the **O**-crystal. For example, the S_0/T_1 SOC value at 273 K for the monomer is 2.54 cm^{-1} (monomer) whereas it is 51.1 cm^{-1} for the face-to-face dimer. In addition, ISC of the dimer is greater than that of the monomer (Figure S32). Moreover, the SOC values also depend on the distance between trityl cation and PF_6 anion, as reflected by the increase in the S_0/T_1 SOC value to 80.2 cm^{-1} at 83 K (Figure S33). These results indicate that the face-to-face cation dimer structural arrangement has a drastic effect on photophysical properties and that the temperature tunable distance between the cation and anion enables control of the emission properties.

Conclusion

In the investigation described above, we uncovered the unique optical nature of the non-substituted trityl cation, which is a fundamental aromatic hydrocarbon cation. The studies show that crystalline trityl PF_6 exhibits a crystal phase transition from **Y**- to **O**-crystals dominated by Ostward's step rule. The unique structure of face-to-face trityl cation dimer in **O**-crystal is stabilized by the arrangement of sextuple phenyl embrace. In addition, trityl PF_6 displays crystalline state fluorescence and phosphorescence. Importantly, the molecular arrangement of the trityl cation and PF_6 anion in the crystalline state plays a dominant role in governing photophysical properties (Figure 10). This phenomenon was explored by using TD-DFT as well as SOC calculations, which gave a more detailed understanding of how ion arrangements in the **Y**- and **O**-crystals govern excited state properties. We believe that other

hydrocarbon cations have the potential of possessing these unique optical properties. It is anticipated that the results of the current effort will pave the way to an exploration of hydrocarbon cations and their use in organic luminescent devices, and in switching and sensing systems.

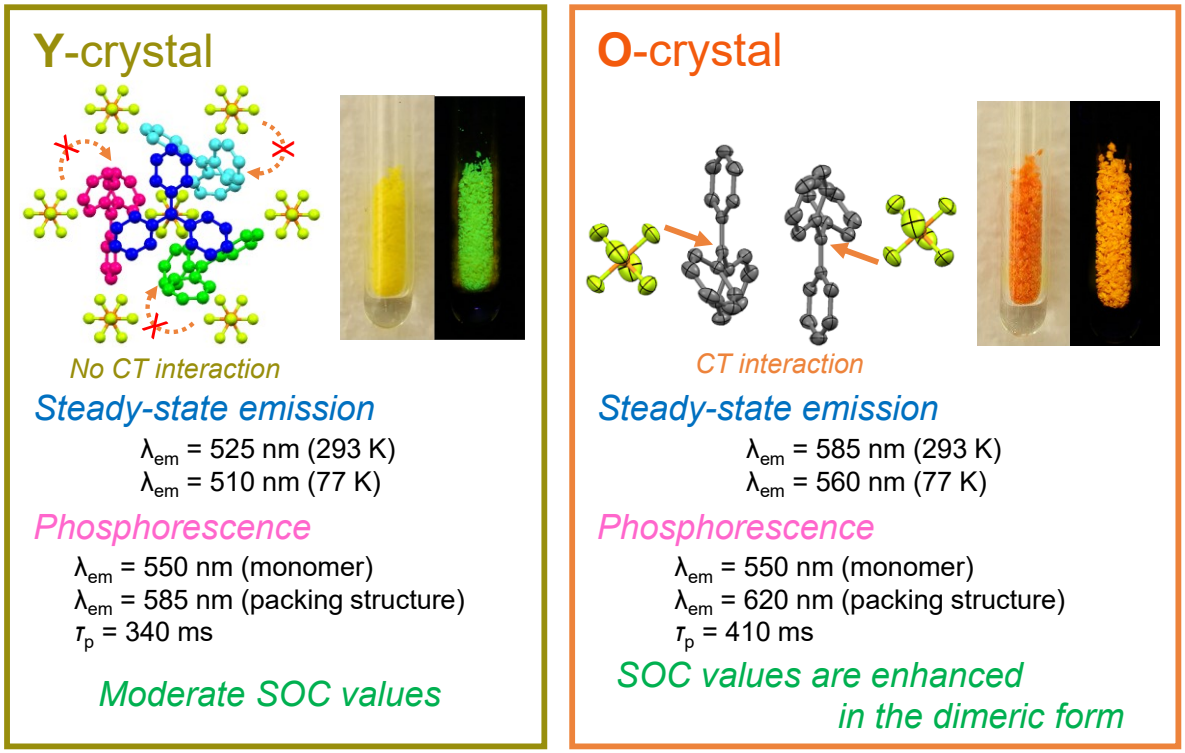

Figure 10. Summary of the relationship between the crystal structures and its photophysical properties in **Y**- and **O**-crystal.

Experimental Section

[CCDC 2063083-2063287 and 2093998 contains the supplementary crystallographic data for this paper. These data can be obtained free of charge from The Cambridge Crystallographic Data Centre via www.ccdc.cam.ac.uk/data_request/cif.]

Acknowledgements

Triphenylmethanol used for the synthesis of the trityl cation was provided by an experimental class of bachelor students in Department of Chemistry, Osaka University. T. N. would like to

thank Prof. Takumi Konno and Prof. Nobuto Yoshinari (Osaka Univ.) for helping to measure emission and excitation spectra, Prof. Shuichi Suzuki (Osaka Univ.) for helping to measure DSC, and Prof. Yasutaka Kitagawa (Osaka Univ.) for fruitful discussions to calculate and evaluate the SOCs of trityl cations. The single crystal X-ray analyses were performed at the Analytical Instrument Facility, Graduate School of Science, Osaka University. The computations were performed at the Research Center for Computational Science, Okazaki, Japan. This study was supported by JSPS KAKENHI Grant-in-Aid for Scientific Research (C), Grant Number JP20K05475 (T.N.) and for Scientific Research (B), Grant Number JP21H01887 (K.K.).

Received: ((will be filled in by the editorial staff))
Revised: ((will be filled in by the editorial staff))
Published online: ((will be filled in by the editorial staff))

References

[1] Reviews: "*Arylcarbonium Ions*": H. H. Freedman, Carbonium Ions, Vol. IV (Eds.: G. A. Olah, P. von R. Schleyer), Wiley-Interscience, New York, 1972, pp. 1501.

[2] J. F. Norris, *Am. Chem. J.* **1901**, *25*, 117.

[3] F. Kehrmann, F. Wentzel, *Ber. Dtsch.Chem. Ges.* **1901**, *34,* 3815.

[4] A. Baeyer, V. Villiger, *Ber. Dtsch.Chem. Ges*. **1902**, *35*, 1189.

[5] G. A. Olah, Q. Liao, J. Casanova, R. Bau, G. Rasul, G. K. S. Prakash, *J. Chem. Soc. Perkin Trans. 2.* **1998**, 2239.

[6] S. Ito, N. Morita, T. Asao, *Bull. Chem. Soc. Jpn.* **1995**, *68*, 1409.

[7] Y. Nishimae, H. Kurata, M. Oda, *Angew. Chem. Int. Ed.* **2004**, *43*, 4947.

[8] T. Nishiuchi, S. Aibara, T. Kubo, *Angew. Chem. Int. Ed.* **2018**, *57*, 16516.

[9] D. F. Duxbury, *Chem. Rev.* **1993**, *93*, 381.

[10] V. Nair, S. Thomas, S. C. Mathew, K. G. Abhilash, *Tetrahedron.* **2006**, *62*, 6731.

[11] T. Gessner, U. Mayer, "Triarylmethane and Diarylmethane Dyes" *Ullmann's Encyclopedia of Industrial Chemistry*, Wiley-VCH, Weinheim, 2000.

[12] S. Kobayashi, M. Murakami, T. Mukaiyama, *Chem. Lett*. **1985**, *14*, 1535.

[13] T. Mukaiyama, M. Tamura, S. Kobayashi, *Chem. Lett*. **1986**, *15*, 1017.

[14] C. J. Urch, "*Triphenylmethyl Hexafluorophosphate*" In Encyclopedia of Reagents for Organic Synthesis, 2001.

[15] M. E. Jung, R. Lagoutte, U. Jahn, "*Triphenylcarbenium Tetrafluoroborate*" In Encyclopedia of Reagents for Organic Synthesis, 2011.

[16] M. S. Shchepinov, V. A. Korshun, *Chem. Soc. Rev*. **2003**, *32*, 170.

[17] R. R. Chance, R. H. Baughman, H. Müller, C. J. Eckhardt, *J. Chem. Phys.* **1977**, *67*, 3616.

[18] E. Hadjoudis, I. M. Mavridis, *Chem. Soc. Rev*. **2004**, *33*, 579.

[19] Y. Morita, S. Suzuki, K. Fukui, S. Nakazawa, H. Kitagawa, H. Kishida, H. Okamoto, A. Naito, A. Sekine, Y. Ohashi, M. Shiro, K. Sasaki, D. Shiomi, K. Sato, T. Takui, K. Nakasuji, *Nat. Mater*. **2008**, *7*, 48.

[20] T. Kinuta, T. Sato, N. Tajima, R. Kuroda, Y. Matsubara, Y. Imai, *J. Mol. Struct.* **2010**, *982*, 45.

[21] X. Sun, B. Zhang, X. Li, C. O. Trindle, G. Zhang, *J. Phys. Chem. A*. **2016**, *120*, 5791.

[22] S. Hirata, *Adv. Opt. Mater.* **2017**, *5*, 1700116.

[23] J. Wang, X. Gu, H. Ma, Q. Peng, X. Huang, X. Zheng, S. H. P. Sung, G. Shan, J. W. Y. Lam, Z. Shuai, B. Z. Tang, *Nat. Commun*, **2018**, *9*, 2963.

[24] K. C. Chen, B. Liu, *Nat. Commun*. **2019**, *10*, 2111.

[25] Y. Tani, M. Terasaki, M. Komura, T. Ogawa, *J. Mater. Chem. C.* **2019**, *7*, 11926.

[26] G. A. Olah, J. J. Svoboda, J. A. Olah, *Synthesis.* **1972**, 544.

[27] J. Bernstein, "*Polymorphism in Molecular Crystals*" Oxford Univ. Press 2002.

[28] T. Mutai, H. Sato, K. Araki, *Nat. Mater*. **2005**, *4*, 685.

[29] S. Kobatake, S. Takami, H. Muto, T. Ishikawa, M. Irie, *Nature.* **2007**, *446*, 778.

[30] I. Halasz, *Cryst. Growth Des.* **2010**, *10*, 2817.

[31] H. Ito, M. Muromoto, S. Kurenuma, S. Ishizuka, N. Kitamura, H. Sato, T. Seki, *Nat. Commun.* **2013**, *4*, 2009.

[32] T. Seki, K. Sakurada, H. Ito, *Angew. Chem. Int. Ed.* **2013**, *52*, 12828.

[33] A. Hinz, R. Labbow, F. Reiss, A. Schulz, K. Sievert, A. Villinger, *Struct. Chem*. **2015**, *26*, 1641.

[34] W. Ostwald, *Z. Phys. Chem*. **1879**, *22*, 289.

[35] R. A. Van Santen, *J. Phys. Chem.* **1984**, *88*, 5768.

[36] T. Threlfall, *Org. Proc. Res. Dev.* **2003**, *7*, 1017.

[37] K. Asai, A. Fukazawa, S. Yamaguchi, *Chem. Eur. J.* **2016**, *22*, 17571.

[38] K. Asai, A. Fukazawa, S. Yamaguchi, *Angew. Chem. Int. Ed*. **2017**, *56*, 6848.

[39] A. Samanta, K. R. Gopidas, P. K. Das, *J. Phys. Chem*. **1993**, *97*, 1583.

[40] R. Deans, J. Kim, M. R. Machacek, T. M. Swager, *J. Am. Chem. Soc.* **2000**, *122*, 8565.

[41] J. Luo, Z. Xie, J. W. Y. Lam, L. Cheng, H. Chen, C. Qiu, H. S. Kwok, X. Zhan, Y. Liu, D. Zhu, B. Z. Tang, *Chem. Commun*. **2001**, 1740.

[42] B. K. An, S. D. Kwon, S. D. Jung, S. Y. Park, *J. Am. Chem. Soc*. **2002**, *124*, 14410.

[43] M. Shimizu, Y. Takeda, M. Higashi, T. Hiyama, *Angew. Chem. Int. Ed*. **2009**, *48*, 3653.

[44] M. Shimizu, T. Hiyama, *Chem. Asian. J.* **2010**, *5*, 1516.

[45] T. Nishiuchi, K. Tanaka, Y. Kuwatani, J. Sung, T. Nishinaga, D. Kim, M. Iyoda, *Chem. Eur. J*. **2013**, *19*, 4110.

[46] T. Nishiuchi, M. Iyoda, *Bull. Chem. Soc. Jpn*. **2014**, *87*, 960.

[47] J. Mei, N. L. C. Leung, R. T. K. Kwok, J. W. Y. Lam, B. Z. Tang, *Chem. Rev*. **2015**, *115*, 11718.

[48] J. Wang, X. Gu, P. Zhang, X. Huang, X. Zheng, M. Chen, H. Feng, R. T. K. Kwok, J. W. Y. Lam, B. Z. Tang, *J. Am. Chem. Soc*. **2017**, *139*, 16974.

[49] The 1D chains of trityl cations are alternatively aligned in opposite directions and the distance between the 1D chains is 7.127 Å (195 K). The alignment and distance those at other temperatures are shown in Figure S6 and S7.

[50] Y. S. Rosokha, S. V. Lindeman, S. V. Rosokha, J. K. Kochi, *Angew. Chem. Int. Ed*. **2004**, *43*, 4650.

[51] B. L. Schottel, H. T. Chifotides, K. R. Dunbar, *Chem. Soc. Rev.* **2008**, *37*, 68.

[52] A. Frontera, P. Gamez, M. Mascal, T. J. Mooibroek, J. Reedijk, *Angew. Chem. Int. Ed.* **2011**, *50*, 9564.

[53] M. Giese, M. Albrecht, K. Rissanen, *Chem. Rev.* **2015**, *115*, 8867.

[54] We thank one of referees for suggesting the existence of SPE interaction in trityl PF_6 dimer.

[55] I. Dance, M. Scudder, *J. Chem. Soc., Chem. Commun.* **1995**, 1039.

[56] I. Dance, M. Scudder, *Chem. Eur. J.* **1996**, *2*, 481.

[57] I. Dance, M. Scudder, *CrystEngComm.* **2009**, *11*, 2233.

[58] By exploring a molecule with triangle shape showing the SPE in crystal, it was found that non-substituted triphenylborane, which is the isoelectronic isomer of trityl cation, also exhibits the SPE, see; F. Zettler, H. D. Hausen, H. Hess, *J. Organomet. Chem.* **1974**, *72*, 157.

[59] K. Okuno, Y. Shigeta, R. Kishi, M. Nakano, *Chem. Phys. Lett.* **2013**, *585*, 201.

[60] C. A. Parker, C. G. Hatchard, *Trans. Faraday Soc*. **1961**, *57*, 1894.

[61] A. Maciejewski, M. Szymanski, R. P. Steer, *J. Phys. Chem*. **1986**, *90*, 6314.

[62] A. Endo, K. Sato, K. Yoshimura, T. Kai, A. Kawada, H. Miyazaki, C. Adachi, *Appl. Phys. Lett.* **2011**, *98*, 083302.

[63] H. Uoyama, K. Goushi, K. Shizu, H. Nomura, C. Adachi, *Nature*. **2012**, *492*, 234.

[64] T. Hatakeyama, K. Shiren, K. Nakajima, S. Nomura, S. Nakatsuka, K. Kinoshita, J. Ni, Y. Ono, T. Ikuta, *Adv. Mater*. **2016**, *28*, 2777.

[65] Z. Yang, Z. Mao, Z. Xie, Y. Zhang, S. Liu, J. Zhao, J. Xu, Z. Chi, M. P. Aldred, Chem. Soc. Rev. 2017, 46, 915.

[66] The reason for the absence of an emission peak λ_{em} = 510 nm originating from the trityl cation monomer in **O**-crystal at 77 K is the occurrence of self-absorption, which is confirmed by viewing the excitation spectra shown in Figure 6c and Figure 9c.